Final Technical Report

Project Title: **Selective Adsorption of Sodium Aluminum Fluoride Salts from Molten Aluminum**

DOE Award Number: DE-FC36-00ID13899

Project Period: 06/01/2000 to 12/31/2004

Principal Investigator: Leonard S. Aubrey
Tel: (828) 697-2411, extension 3316
E-mail Address: laubrey@selee.com

Recipient Organization: SELEE Corporation
700 Shepherd Street
Hendersonville, NC 28792

Subcontractors: Alcoa Technical Center
Ingot and Solidification
Alcoa, PA

Acknowledgment: This report is based on work supported by the U.S. Department of Energy under Award Number DE-FC07-00ID13899

Table of Contents

List of Tables and Figures

Figure 12: Results of mercury porosimetry analysis of the SBA micro-porous filter media before and filtration showing the change in micro-porosity due to capillary adsorption of the sodium aluminum fluoride bath.

Figure 13: Backscatter electron image of used sintered bonded alumina micro-porous filter media. Figure 14 contains an EDS analyses made at equi-distance locations across the center from left to right.

Figure 14: Results of equi-distance EDS analyses made across the SBA micro-porous filter section shown in Figure 13.

Figure 15: Photograph of used dense alumina ball. Figure 16 contains of EDS analyses made at equi-distance locations across the center from left (starting on adhering chiolite layer) to right.

Figure 16: Results of equi-distance EDS analyses made across the used dense alumina ball section shown in Figure 15. EDS results obtained to the left of vertical dashed line were made inside the adhering bath layer. EDS results to the right of the vertical dashed line were made inside the dense alumina ball.

Selective Adsorption of Sodium aluminum Fluoride Salts from Molten Aluminum

Leonard S. Aubrey[1], Christine A. Boyle[2], Eddie M. Williams[3], David H. DeYoung[4], Dawid D. Smith[5], Feng Chi[1]

[1] SELEE Corporation, 700 Shepherd Street, Hendersonville, NC, 28792, USA
[2] Consultant, White Oak, Pennsylvania, 15131, USA
[3] Alcoa Warrick Operations, Newburgh, Indiana, 47629, USA
[4] Alcoa Inc., Alcoa Technical Center, 100 Technical Drive, Alcoa Center, PA, 15069, USA
[5]Consultant, Hendersonville, NC, 28792, USA

Executive Summary

Aluminum is produced in electrolytic reduction cells where alumina feedstock is dissolved in molten cryolite (sodium aluminum fluoride) along with aluminum and calcium fluorides. The dissolved alumina is then reduced by electrolysis and the molten aluminum separates to the bottom of the cell. The reduction cell is periodically tapped to remove the molten aluminum. During the tapping process, some of the molten electrolyte (commonly referred as "bath" in the aluminum industry) is carried over with the molten aluminum and into the transfer crucible. The carryover of molten bath into the holding furnace can create significant operational problems in aluminum cast houses. Bath carryover can result in several problems. The most troublesome problem is sodium and calcium pickup in magnesium-bearing alloys. Magnesium alloying additions can result in Mg-Na and Mg-Ca exchange reactions with the molten bath, which results in the undesirable pickup of elemental sodium and calcium.

This final report presents the findings of a project to evaluate removal of molten bath using a new and novel micro-porous filter media. The theory of selective adsorption or removal is based on interfacial surface energy differences of molten aluminum and bath on the micro-porous filter structure. This report describes the theory of the selective adsorption-filtration process, the development of suitable micro-porous filter media, and the operational results obtained with a micro-porous bed filtration system.

The micro-porous filter media was found to very effectively remove molten sodium aluminum fluoride bath by the selective adsorption-filtration mechanism. Liquid bath was never visually observed downstream of the bed filter using any of the bed packing configurations used in this investigation. The performance of the various filter configurations was assessed by the increase in soluble sodium from a magnesium-bath reversion reaction test. The lowest average sodium increase (1 ppm) was obtained with the micro-porous filter media compared to no media (4 ppm), balls only (7 ppm), and no filter (4 ppm) bed configurations. The lower average sodium pickup values obtained with the micro-porous filter media compared to the other bed filter configuration were statistically significant at a 95% confidence level.

SEM/EDS analysis and mercury intrusion porosimetry of the used micro-porous filter media confirmed that molten bath (chiolite) was removed by selective adsorption. The interior of the micro-porous filer media was nearly fully saturated with chiolite bath. Very little adhering bath was observed on the surface of the used micro-porous media.

Introduction

Aluminum is produced in electrolytic reduction cells where alumina feedstock is dissolved into molten cryolite (sodium aluminum fluoride) along with aluminum fluoride and calcium fluoride. The dissolved alumina is then reduced by electrolysis and the molten aluminum separates to the bottom of the cell. The reduction cell is then periodically tapped to remove the molten aluminum. During the tapping process, some of the molten electrolyte (commonly referred as "bath" in the aluminum industry) is carried over with the molten aluminum and into the transfer crucible. Bath is an insoluble contaminant that needs to be removed prior to transfer into the holding furnace. Ideally the molten bath in the transfer crucible is allowed to cool and solidify. The solid bath "crust" is then removed by thorough skimming. In actual practice, these conditions are rarely achieved on a consistent basis.

The carryover of molten bath into the holding furnace can create significant operational problems in aluminum cast houses. Bath carryover can result in the following problems:

1. Build-up of a bath crust or residue on the holding furnace walls.

2. In the case of magnesium-bearing alloys, the magnesium alloying addition can result in Mg-Na and Mg-Ca exchange reactions between the metal and the bath. The result is pickup of elemental sodium and calcium impurities in the molten aluminum [1]:

$$2(Na_3AlF_6) + 3Mg \rightarrow 6Na + 2AlF_3 + 3MgF_2$$

and

$$CaF_2 + Mg \rightarrow Ca + MgF_2$$

This exchange reaction is called reversion. These impurities can result in edge cracking during subsequent ingot rolling, and therefore chlorine fluxing must be employed to reduce the soluble alkali level down to an acceptable level. In the case of direct chill billet casting, higher levels of sodium have been reported to result in increased pit scrap. Chlorine fluxing in the holding furnace results in a significant loss in furnace productivity as well as environmental, safety, and energy concerns.

This report summarizes the findings of a project to evaluate whether a micro-porous filter media could be used to remove the molten bath by selective adsorption. This project was a partnership between SELEE Corporation, the Alcoa Technical Center, and the Office of Energy Efficiency and Renewable Energy of the U. S. Department of Energy.

Theory of Selective Adsorption Filtration

The removal of molten bath is a liquid-liquid-solid separation process. Filtration is an accepted technology in aluminum cast houses for removal of insoluble solid impurities in molten aluminum. The removal of a liquid inclusion is dependent on the work of adhesion between the liquid inclusion and the filter substrate material. The work of adhesion is dependent on the interfacial surface energies between three components:

1. Molten metal (m)
2. Molten bath (l)
3. Filter material (f)

The degree of wetting between either the molten aluminum or molten bath and the filter material is denoted by the contact-wetting angle (θ), which is schematically illustrated in Figure 1. Whether a liquid inclusion will adhere to a filter substrate surface is dependent on the work of adhesion (WA_{lf}) [2]:

$$WA_{lf} = \gamma_{mi}(1+ \cos\theta_{lf\text{-}lm})$$

$\theta_{lf\text{-}lm}$ = contact wetting angle between the liquid inclusion and the filter

γ_{ml} = interfacial surface energy between the metal and liquid inclusion

The work of adhesion is maximized at a low contact-wetting angle between the filter substrate and the molten bath. Dense filter materials such as ceramic foam or tabular alumina grain or balls in bed filters have limited capacity to retain liquid bath because of limited interconnected micro-porosity. As a result bath retention is limited to the external surface area of the ceramic filter media. A bed filter can overcome this limitation to some extent by its large size and therefore large surface area. After the filter surface becomes completely covered or saturated with liquid inclusion material, filtration transitions to mode where the filter acts to coalesce small liquid inclusions and release larger liquid inclusion particles back into the metal. The proposed technical solution for bath removal is to utilize a micro-porous filter media designed to preferentially adsorb the molten bath by capillary action [3]. This is accomplished by developing a micro-porous filter media where there is a large difference between the contact wetting angles of molten aluminum and molten bath on the micro-porous filter material (i.e. aluminum has a high wetting angle on the filter material and bath has a low wetting angle). The required head pressure (H_P) for capillary penetration of a micro-porous ceramic is defined by [5]:

$$H_p = -4\cdot\gamma_{ls}\cdot\cos(\theta_{ls})/\rho_l\cdot g.\phi$$

Where: Hp = metallostatic head pressure required for capillary penetration into the micro-porous filter media

γ_{ls} = interfacial surface energy between the liquid phase (bath or aluminum) and the micro-porous filter media

θ_{ls} = contact angle between the liquid phase (bath or aluminum) and the micro-porous filter media

ρ_l = density of the surrounding liquid phase
g = Newton's gravitational constant

ϕ = critical pore size of the micro-porous filter media

For effective bath adsorption, the micro-porous filter must be non-wetting by the molten aluminum such that the molten aluminum cannot penetrate into the fine micro-porous structure, while at the same time the bath must be wetting to the filter material. Effective adsorption therefore requires a large difference in contact wetting angle between metal-filter and bath-filter material. Figure 2 schematically illustrates the concept of selective adsorption of bath from molten aluminum.

Utigard et. al. [6] utilized the sessile drop technique to determine the interfacial tensions in the ternary system of cryolite, alumina and aluminum and reported a contact angle of 158^o between the alumina and the molten aluminium and a contact angle of 22^o between the alumina and cryolite. Dewing et. al. [7] reported contact angles of 177^o for molten aluminium on alumina and 3^o for molten cryolite on alumina using a capillary depression technique. These large contact wetting angle differences reported in literature between the metal-filter and bath-filter materials indicates that micro-porous alumina should be able to effectively separate molten bath from molten aluminum by preferential adsorption.

Development of Micro-Porous Filter Materials

Two types of micro-porous filter materials were developed. The first material was sinter-bonded alumina (SBA) using fine, activated alumina as a binder. After high temperature firing, this material obtained a 100% α-Al_2O_3 microstructure. The second material was glass-frit bonded alumina (FBA). The frit material was CaO-MgO-Al_2O_3-B_2O_3 glass that is highly non-wetting to molten aluminum. The sacrificial pore forming material in both materials were hollow polymer micro-spheres with a nominal diameter of 80 microns. The physical size of the media was 4 mm diameter by 10 to 12 mm in length and was produced by an extrusion process. The overall open porosity was 70 to 80%. Figure 3 shows the pore size distribution of the SBA micro-porous filter material that was determined by mercury intrusion porosimetry (MIP). The pore diameter of the porosity averaged about 80-microns. The connecting window diameter between pores ranged between 10 and 25 microns. The micro-porous material is shown in Figures 4 and 5.

Molten Metal Evaluation

The technical feasibility of removing molten bath by selective adsorption using micro-porous filtration was evaluated at the Alcoa Technical Center. Figure 6 is a schematic illustration of the experimental casting station used to evaluate the effectiveness of the micro-porous filter media. The casting station consisted of a 900 kg induction furnace used to simulate the transfer crucible. Leading from the induction furnace was a short transfer launder to a crucible bed filter (inlet area =1,100 cm^2) that was gas heated. After the crucible bed filter, the molten metal could flow into either a collection drain pan or gas fired crucible furnace for bath sampling. Hand dams controlled the metal flow after the bed filter to either the crucible furnace or the collection drain pan.

The furnace charge consisted of 680 kg of pure (P0506A) pig. After melting and heating to 960 °C, a mixture of commercial bath (2.6-4% of furnace charge weight) along with AlF_3 was added and stirred in by hand. The main constituent of bath, cryolite (Na_3AlF_6), is located at 25 mol% AlF_3. Typical bath is located between 30 and 35 mol% AlF_3, with an approximate melting temperature of 960 ^oC (Figure 7). As the bath begins to cool, cryolite freezes out first. The remaining liquid bath becomes richer in AlF_3. At 741^oC chiolite ($Na_5Al_3F_{14}$) starts to solidify. Theoretically, liquid bath can be present down to a temperature of 694^oC. These phase transformations are based on a pure NaF-AlF_3 mixture and would be shifted in the presence of other phase constituents. For the experimental test evaluation, additional AlF_3 was added to promote the formation of the lower melting point bath. The AlF_3 addition ranged from 10 to 20% weight percent of the bath addition.

Table 1 outlines the matrix of variables evaluated in the experimental test runs. The details of the bed filter packing are given in Table 2 and in Figure 6. To quantify the amount of bath remaining in the metal after the bed filter, a magnesium-sodium and magnesium-calcium reversion test was run in the heated sampling crucible maintained at 843°C. After approximately 50% of the induction furnace had been poured, the test crucible was filled with approximately 23 kg of metal. After the molten aluminum filled the crucible, a 50% Al-Mg master alloy addition was made to target a magnesium concentration of 5% wt. percent. After the magnesium was added and stirred in, analytical samples were collected every minute for 10 minutes and then again at 15 and 20 minutes. Analytical chill samples were analyzed for sodium and calcium pickup from the reversion reaction of the magnesium with any remaining bath. Figure 8 shows typical Mg-Na reversion test results obtained with alumina balls and sinter-bonded alumina micro-porous filter media.

Results

The metal was poured from the furnace at the fastest rate possible without overflowing the launder system. When the metal was unrestricted (no filter media), the pour time

duration averaged 13 minutes resulting in a pour rate of 48 kg per minute. The pouring rate varied from 48 to 16 kg per minute depending on whether filter media was used and the age of the filter bed media. For the runs where filter media was used, as the number of runs through the media increased, the pour rate decreased. After the ninth run with the sinter bonded alumina micro-porous media, the pour time increased to 40 minutes resulting in a pour rate of 16 kg per minute.

At the two highest tap temperatures, the bath in the induction furnace was liquid and was observed to exit the furnace into the transfer launder leading to the bed filter for the first few minutes of each test run. At the lowest furnace tap temperature, the bath in the induction furnace was solid and very little liquid bath was observed during tapping. During the experimental runs, the metal temperature drop between the induction furnace and the bed filter was 50 to 100 °C.

The sodium pickup results obtained with the various bed filter configurations are shown graphically in Figure 9 and summarized in Table 3. Statistical analysis of the sodium pick-up data showed that there was not a statistically significant difference in the sodium increase as a function of tapping temperature or bed filter temperature. The sodium pick-up was statistically lower for the SBA and FBA micro-porous filter media when compared to the alumina balls only and no bed filter configurations. These statistical analyses were made using "JMP" statistical software at a 95%- confidence level.

The spent micro-porous filter media and the alumina balls were retrieved for further analysis for retained bath. The spent micro-porous filter media was analyzed using mercury intrusion porosimetry, SEM/EDS analysis, and x-ray diffraction.

Figure 10 is a photograph of the used SBA micro-porous filter media. The spent media did not contain any adhering aluminum and was heavily saturated with retained bath. Figure 11 is a secondary electron image showing the surface micro-topography that has a glassy appearance compared to the original porous appearing surface. Figures 10 and 11 can be compared to the original micro-porous surface in Figures 4 and 5. The micro-porous pore size distribution was obtained before and after filtration by mercury intrusion porosimetry to determine the change in porosity due to capillary adsorption of the sodium aluminum fluoride bath. Figure 12 shows the micro-porosity before and after filtration for the SBA micro-porous filter media. Table 4 summarizes the porosimetry results obtained before and after filtration for both types of micro-porous filter media. The porosimetry results indicate a large porosity change as the results bath adsorption, indicating the filter media had been nearly completely infiltrated with bath.

SEM analysis of the FBA material indicated a slight chemical reaction with either the molten aluminum or bath. The SBA material was un-reacted. Figure 13 shows a backscatter electron image of a polished cross section of the used SBA micro-porous material. EDS analyses were obtained across the center of the sample along a horizontal line from left to right. Figure 14 graphically illustrates the results obtained for F, Na, Al

and Ca showing bath penetration or adsorption into the center of the sample. The media appears to be saturated, as there is no gradient from the exterior to the center. The used SBA micro-porous media was analyzed by x-ray diffraction. XRD analysis confirmed the presence of chiolite and α- alumina. Figure 15 shows a cross section of a used alumina ball taken from near the top of the bed. Figure 16 shows the results EDS readings obtained across the sample from left to right starting in the adhering bath layer on the left. Figure 16 shows very little capillary adsorption of the bath into the dense alumina ball.

Conclusions

1. The AlF_3 addition to cyrolite produced a liquid bath similar to that observed in transfer crucibles in aluminum smelters. The liquid bath was not uniformly suspended in the metal in the induction furnace, and during pouring, most of bath was observed only during the first few minutes of transfer. Large amounts of liquid bath was observed at the higher pouring temperatures of 871 °C and 927 °C, but very little liquid bath was observed at the lower pouring temperature of 816 °C. Liquid bath was never observed downstream of bed filter with any of the bed filter configurations.
2. The performance of the various filter configurations was assessed by the increase in sodium from a magnesium-bath reversion reaction test. The lowest average sodium increase (1 ppm) was obtained with the micro-porous filter media compared to no media (4 ppm), balls only (7 ppm), and no filter (4 ppm) bed configurations. The lower average sodium pickup values obtained with the micro-porous filter media compared to the other bed filter configuration were statistically significant at a 95% confidence level.
3. SEM/EDS analysis and mercury intrusion porosimetry of the used micro-porous filter media confirmed that molten bath (chiolite) was removed by selective adsorption. The interior of the micro-porous filter media was saturated with chiolite bath. Very little adhering bath was observed on the surface of the used micro-porous media. Analysis of the dense alumina ball showed very little if any bath penetration into the internal structure of the ball. The bath was observed only on the exterior surface of the ball.

Accomplishments

The technical feasibility of removing immiscible second phase liquid inclusions was demonstrated using a new and novel selective adsorption filtration process. The use of hollow polymer micro-spheres as a pore former in the filter slurry resulted in a high degree of well inter-connected micro-porosity suitable for removing low-wetting angle second phase inclusion material such as molten sodium aluminum fluoride bath.

The global aluminum industry is very active in searching-out, developing and implementing new aluminum treatment processes to effectively remove soluble alkali impurities from molten aluminum. The aluminum industry still relies heavily on chlorine gas treatment to remove soluble sodium and calcium impurities. There is significant environmental, health and safety issues surrounding the transport, storage, handling and use of chlorine in aluminum cast houses. The selective adsorption process could be implement by using the micro-porous filter material in a bed filter-type treatment station located between the smelter and the holding furnace. The selective adsorption process could also be used to complement existing crucible treatment processes where aluminum fluoride is added to remove soluble alkali impurities. These crucible treatment processes can result in the formation of liquid chiolite-rich bath, which if not effectively removed, can result in "bath carryover" type situation.

The selective adsorption process has widespread potential application in refining molten metals beyond the separation of molten sodium aluminum fluoride bath from molten aluminum. The selective adsorption filtration process could be utilized for removing chloride salts generated from in-line degassing systems and as well as holding furnace fluxing salts. In addition the selective adsorption filtration technology could be used to selectively remove complex molten oxide and silicate slags from molten iron and steel.

Publications

The results of this work were presented at the Ninth Australian Conference and Exhibition 12-15 September 2005, in Melbourne, Australia. The paper was published in Conference Proceedings: Aluminum Cast House Conference Technology 2005; Edited by John A. Taylor, Ian F. Bainbridge, and John F. Grandfield; pages 57 – 68; ISBN 0 643 09135-1.

Acknowledgements

The hard work of John Hartill, Charlie Myers, and Bob McCullough of the Alcoa Technical Center in conducting these trials is acknowledged. In addition the contributions made by Angela Withers, Niki Rhodes and Rudy Olson of SELEE Corporation is acknowledged.

References

[1] DeYoung, D. H., "Na And Ca Pickup from Hall Bath in Ingot Furnaces," Light Metals 1997, The Metallurgical Society, Warrendale, PA, 1997

[2] Apelian, D., Luk, S., Piccone, T., and Mutharasan, R., "Removal of Liquid and Solid Inclusions from Steel Melts," Fifth International Iron and Steel Congress, Proceedings of the 69th Steel Making Conference, Vol. 69, 1986, 957 – 967

[3] United States Patent Number 6,036,743, "Method and Apparatus for Removing Liquid Salts from Liquid Metal," K. R. Butcher and L. S. Aubrey, March 14, 2000.

[4] Levin, E. M. and McMurdie, H. F., " Phase Diagrams for Ceramists," Volume III, The American Ceramic Society, 357.

[5] Gauckler, L. J., Waeber, M. M., Conti, C., and Jacob-Duliere, M., "Industrial Application of Open Pore Ceramic Foam for Molten Metal Filtration," Light Metals 1985, The Metallurgical Society, Warrendale, PA, 1261

[6] Utigard, T. and Toguri, J. M., "Interfacial Tension of Aluminum in Cryolite Melts," Volume 16B, Metallurgical Transactions B, June 1985, 333 – 338.

[7] Dewing, E. W. and Desclaux, P., "Interfacial tension of aluminum in cryolite melts saturated with alumina,." Volume 8B, Metallurgical Transactions B, December 1977, page 557.

Table 1: Matrix of Test Variables in Experimental Molten Metal Runs

Filtration Variables	Bed Packing Configuration		Number of Runs
	Alumina balls only in bed		2
	FBA micro-porous media		5
	SBA micro-porous media		9
	No filter media		11
	No bed filter		1
	Bed Filter Temperature	927 °C	
		816 °C	
Metallurgical Variables	Furnace Tapping Temperature	927 °C	
		871 °C	
		816°C	

Table 2: Details of Bed Filter Packing

Layer	Material	Height, mm
Top	20 mm ∅ dense alumina balls	100
Middle	Micro-porous filter media	125
Bottom	20 mm ∅ dense alumina balls	150 (50 above bottom of under flow baffle)

Table 3: Summary of Sodium Pick-up Results from Mg-Bath Reversion Reaction after the 5 Wt. % Magnesium Alloying Addition

Bed Filter Configuration	Sodium Pickup - ppm		
	Minimum	Maximum	Average
No Filter Media	1	10	4
Alumina Balls Only	4	9	7
FBA Micro-Porous Filter	0	2	1
SBA Micro-Porous Filter	0	2	1
No Bed Filter	Only one test point		4

Table 4: Summary of Mercury Porosimetry Intrusion Results Obtained on Micro-Porous Filter Media Before and After Filtration

Micro-Porous Filter Media Type	Before/After Filtration	Median Pore Diameter, μ	Average Pore Diameter, μ	Porosity, %
SBA	Before	11.90	4.11	71.1
	After	1.52	0.38	12.6
FBA	Before	23.87	4.73	79.5
	After	9.56	0.12	16.2

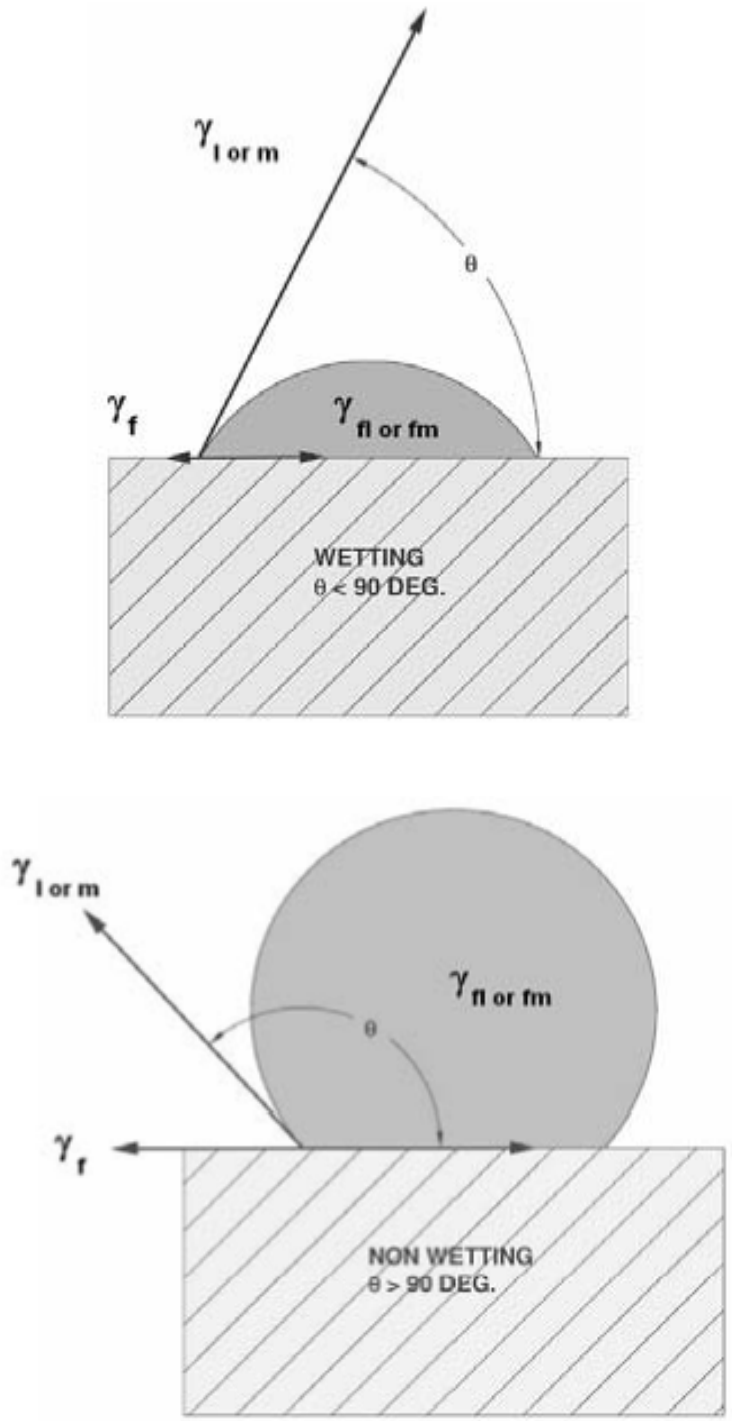

Figure 1: Schematic illustration of interfacial surface energy components for wetting ($\theta < 90°$) and non-wetting ($\theta > 90°$) conditions for molten metal contact on a refractory surface**.**

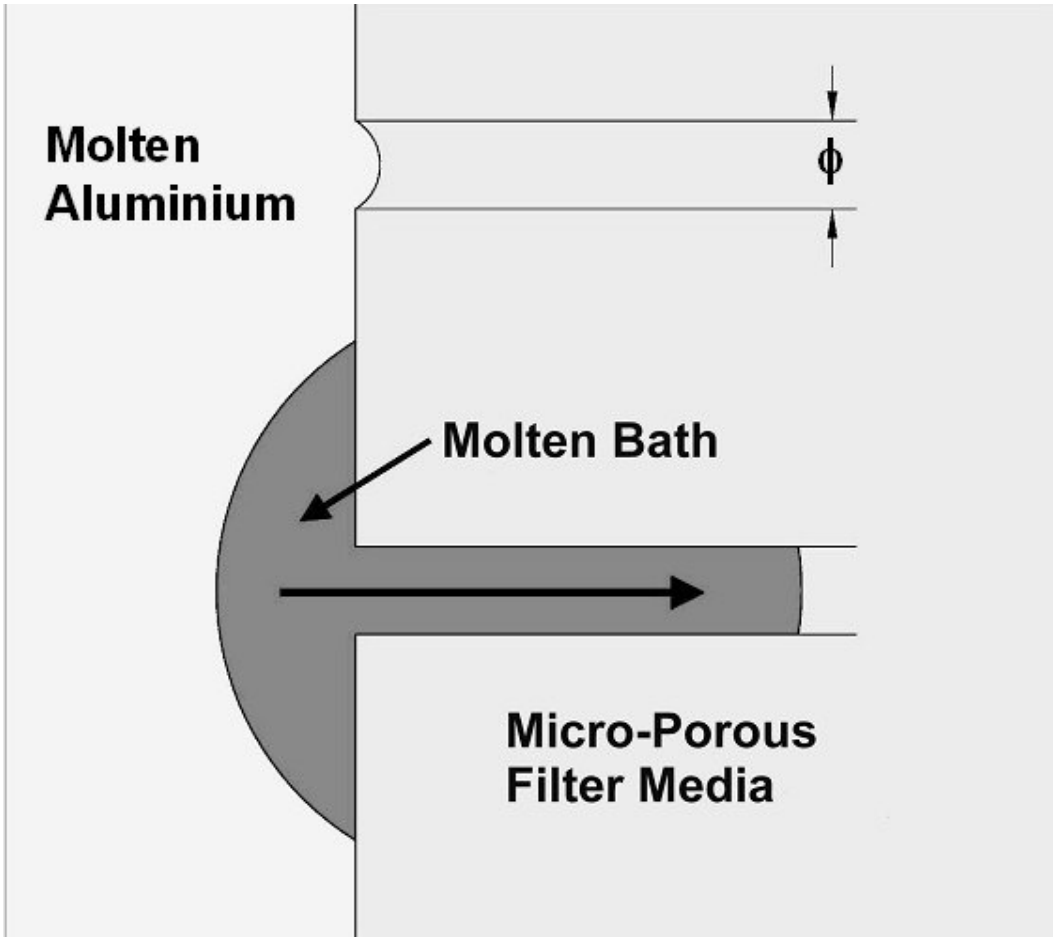

Figure 2: Schematic illustration of selective adsorption of molten bath from molten aluminum using a micro-porous filter.

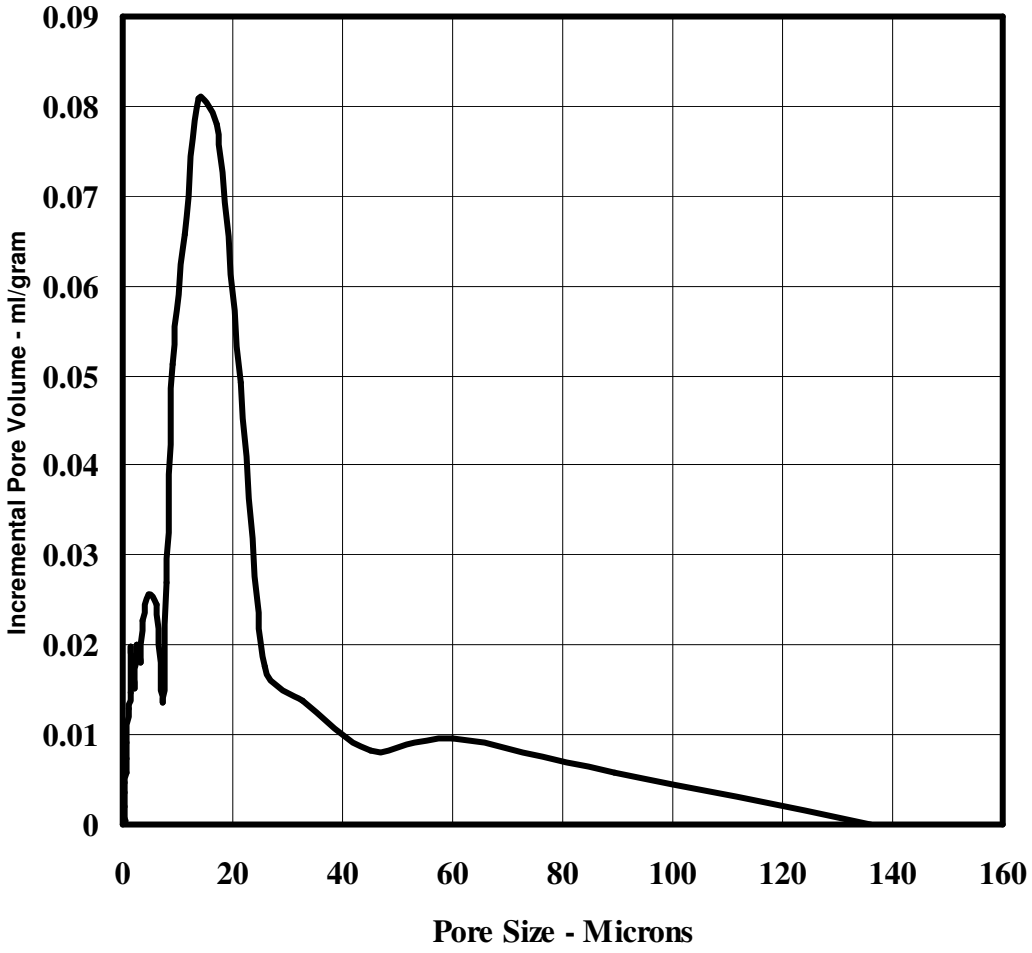

Figure 3: Pore size distribution of sinter bonded alumina (SBA) micro-porous filter media determined by mercury intrusion porosimetry.

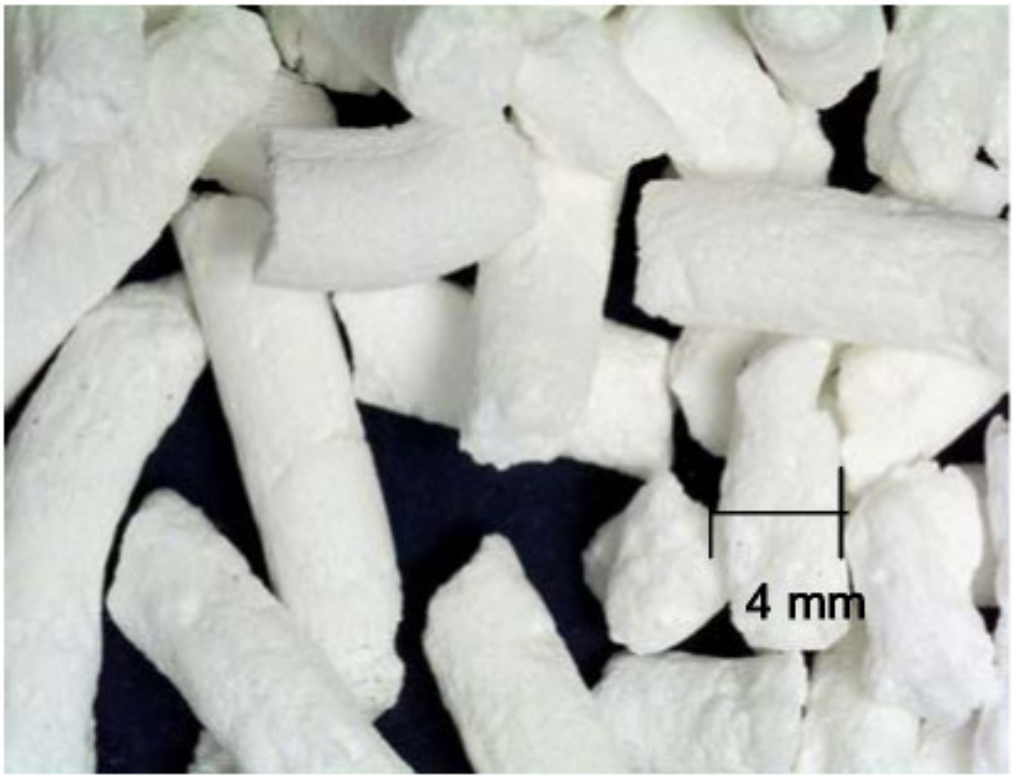

Figure 4: Photograph of SBA micro-porous filter media. Nominal diameter of the media is 4 mm.

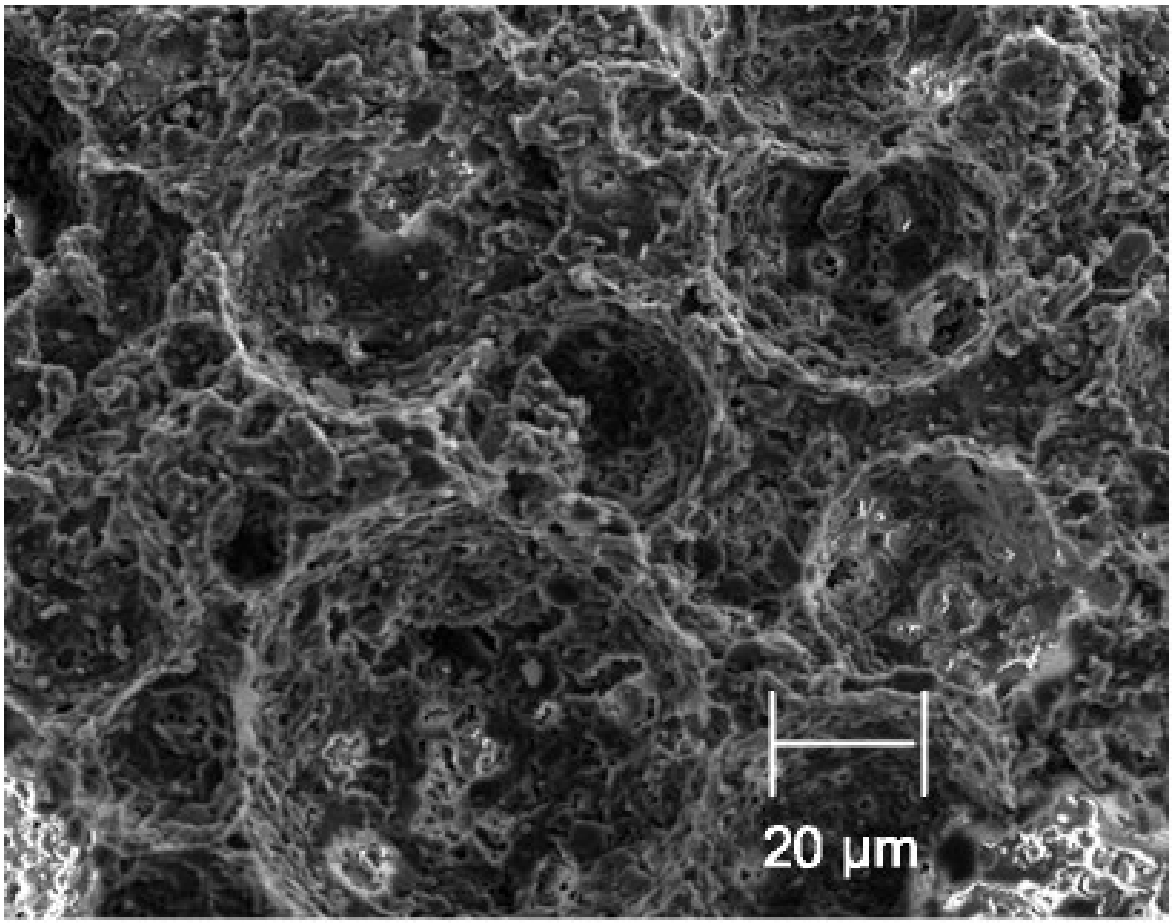

Figure 5: Secondary electron image of SBA micro-porous filter media. Note amount of surface micro-porosity that connects to subsurface micro-porosity.

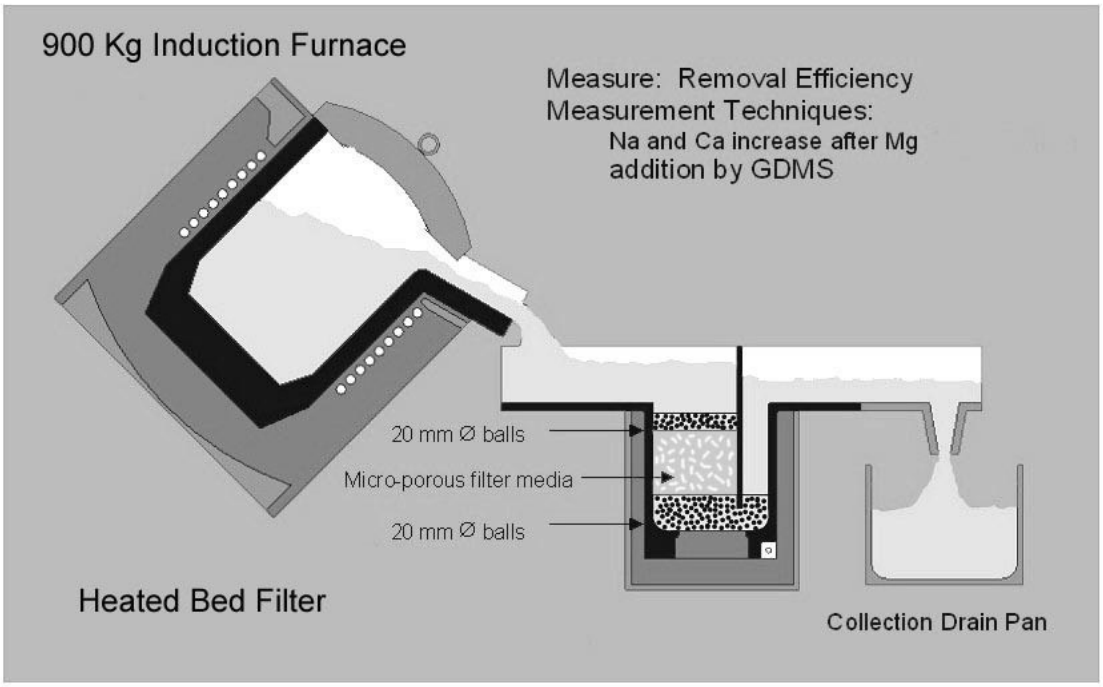

Figure 6: Schematic illustration of experimental casting station used to evaluate bath removal by selective adsorption.

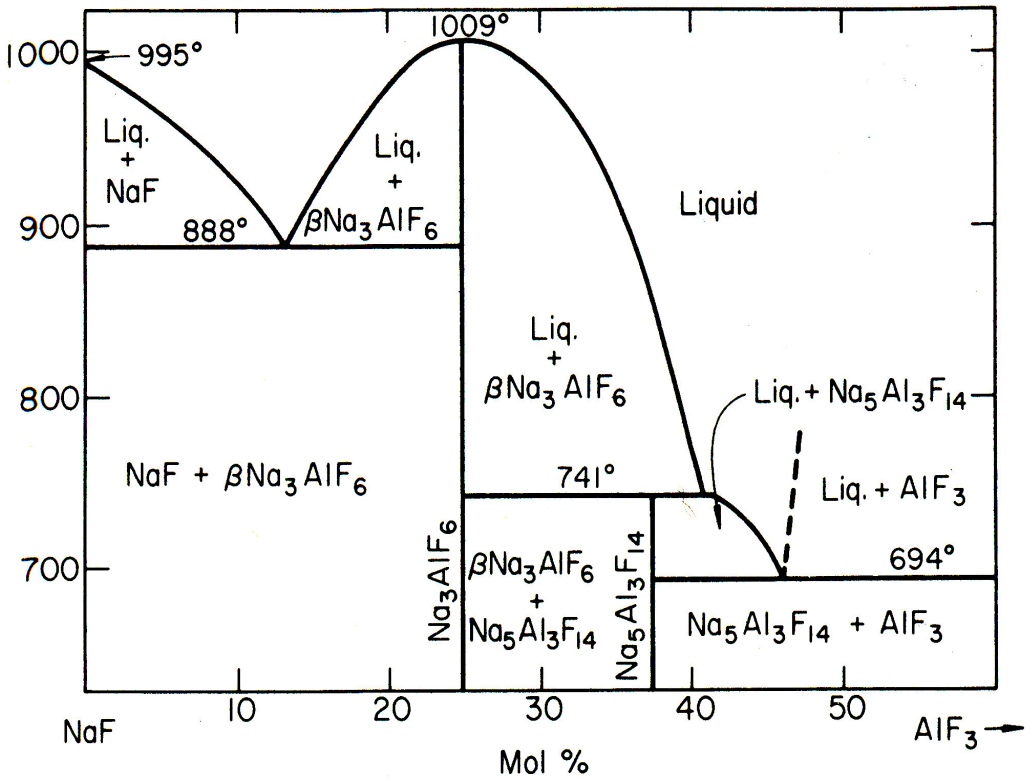

Figure 7: AlF_3 binary phase diagram [4].

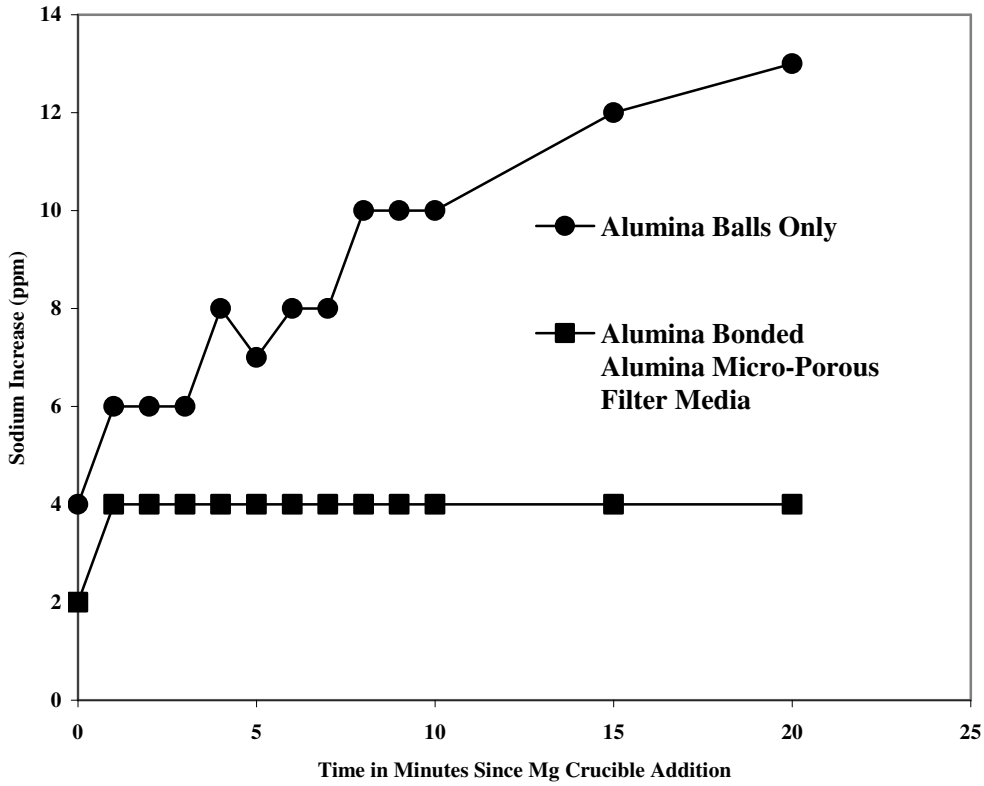

Figure 8: Typical Mg-Na reversion reaction test results obtained in the heated crucible test to determine the amount of bath remaining after filtration.

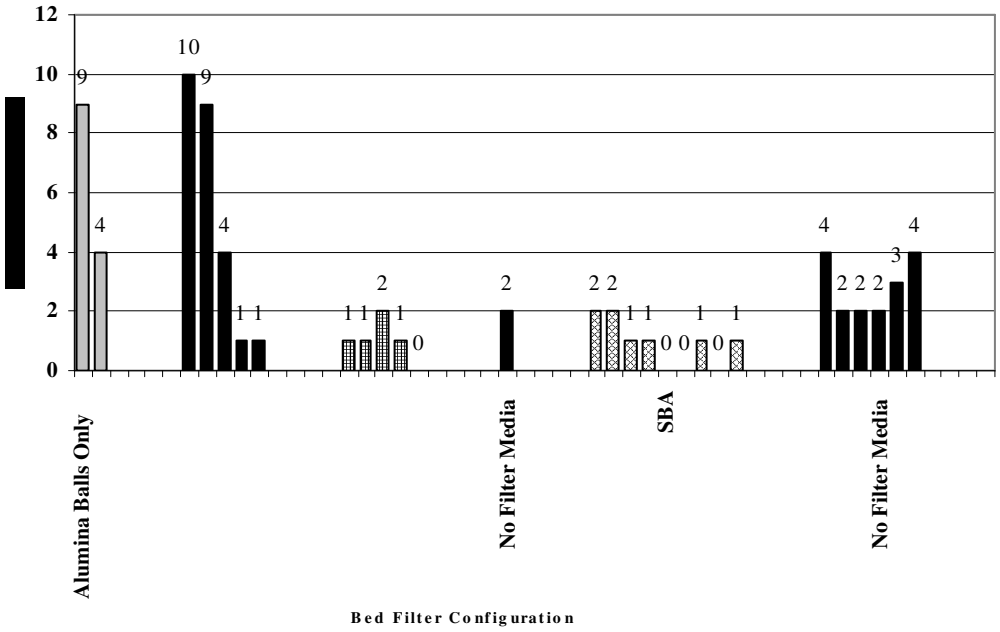

Figure 9: Sodium pickup from Mg-bath reversion reaction designed to determine the effectiveness of the bed filter with various filter media configurations.

Figure 10: SBA micro-porous filter media after removal from bed filter.

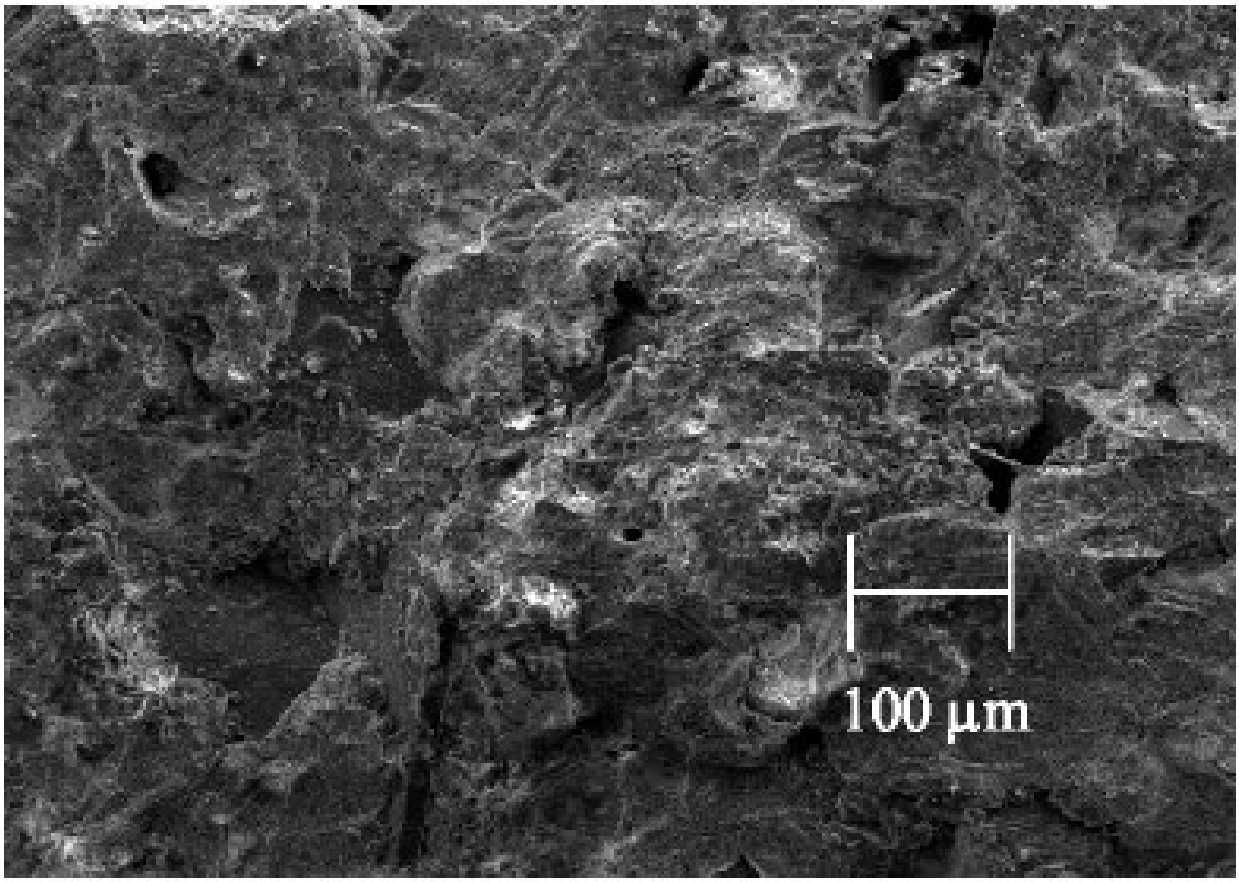

Figure 11: Secondary electron image showing the surface micro-topography of used SBA micro-porous filter media. Compare to Figure 5 for the before filtration condition.

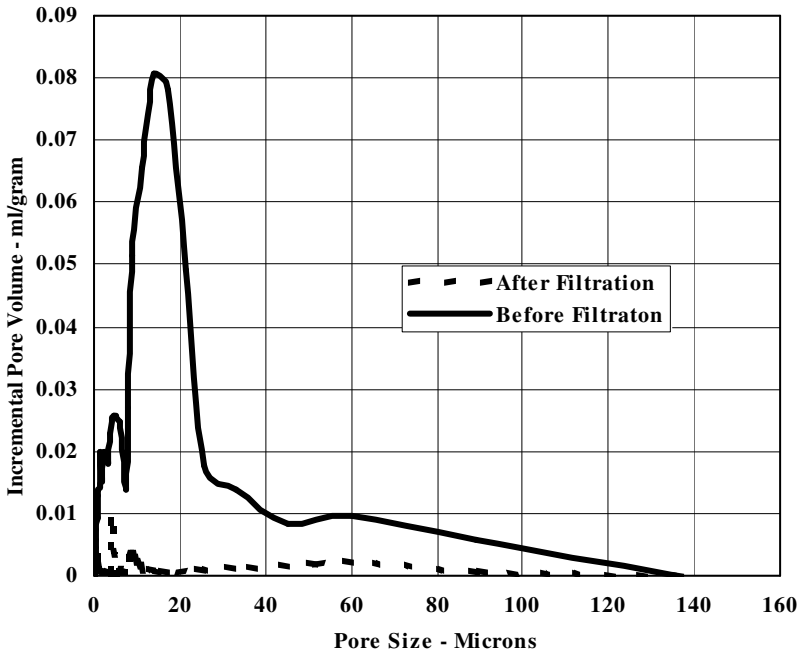

Figure 12: Results of mercury porosimetry analysis of the SBA micro-porous filter media before and after filtration showing the change in micro-porosity due to capillary adsorption of the sodium aluminum fluoride bath**.**

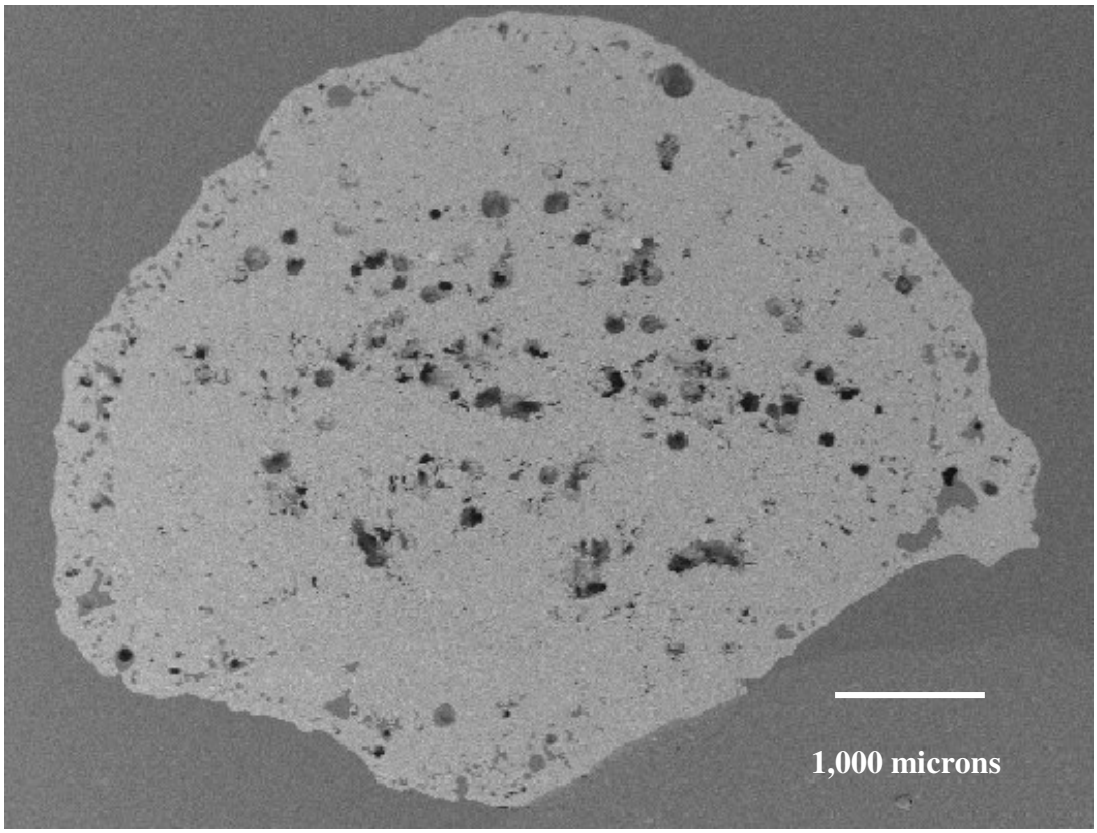

Figure 13: Backscatter electron image of used sintered bonded alumina micro-porous filter media. Figure 14 contains EDS analyses made at equi-distance locations across the center from left to right.

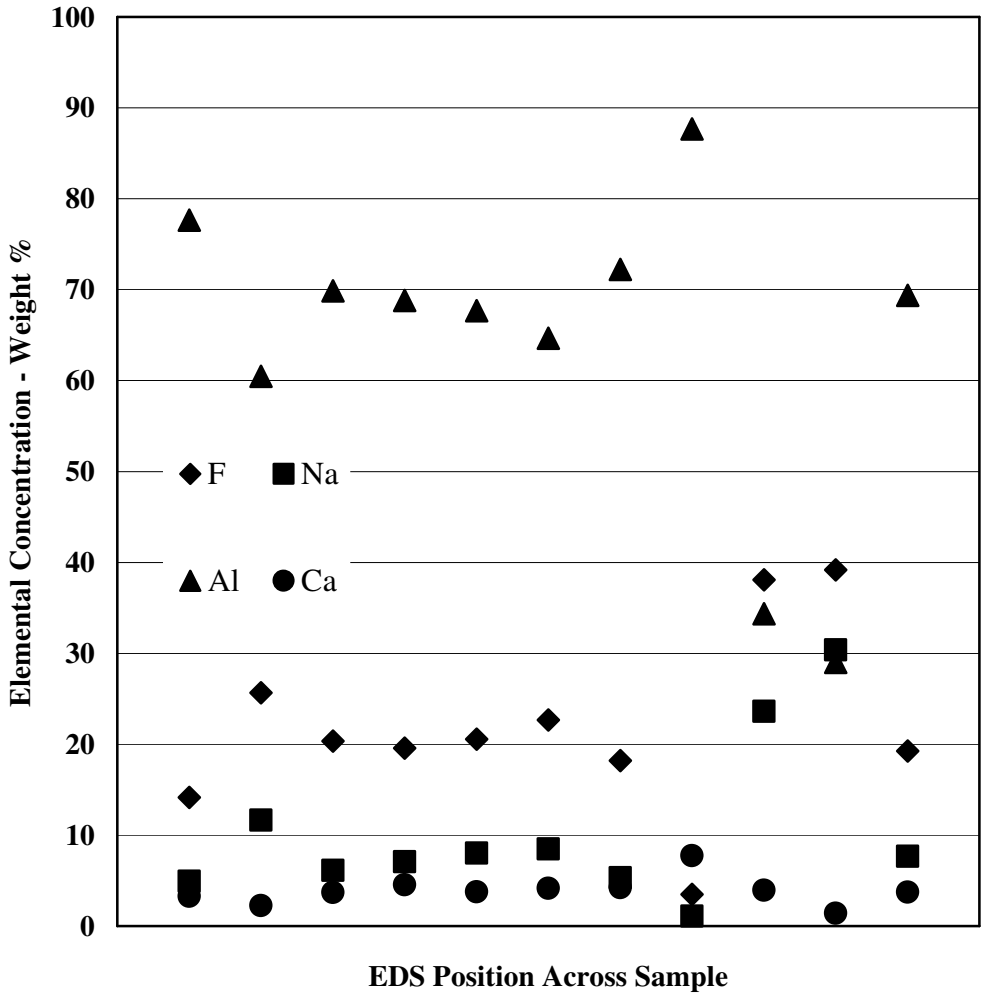

Figure 14: Results of equi-distance EDS analyses made across the SBA micro-porous filter section shown in Figure 13.

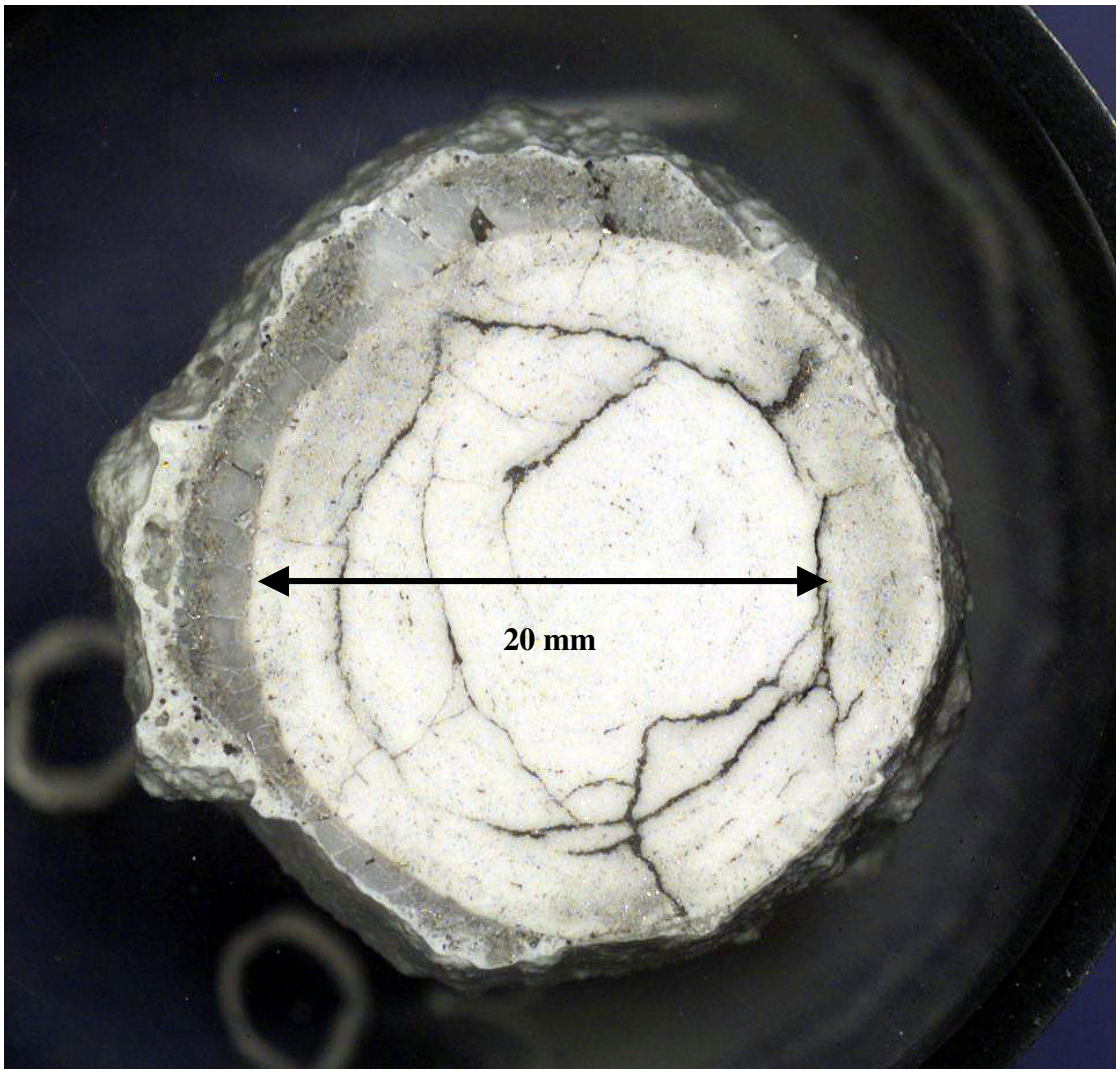

Figure 15. Photograph of used dense alumina ball. Figure 16 contains EDS analyses made at equi—distance locations across the center from left (starting on adhering chiolite layer) to right.

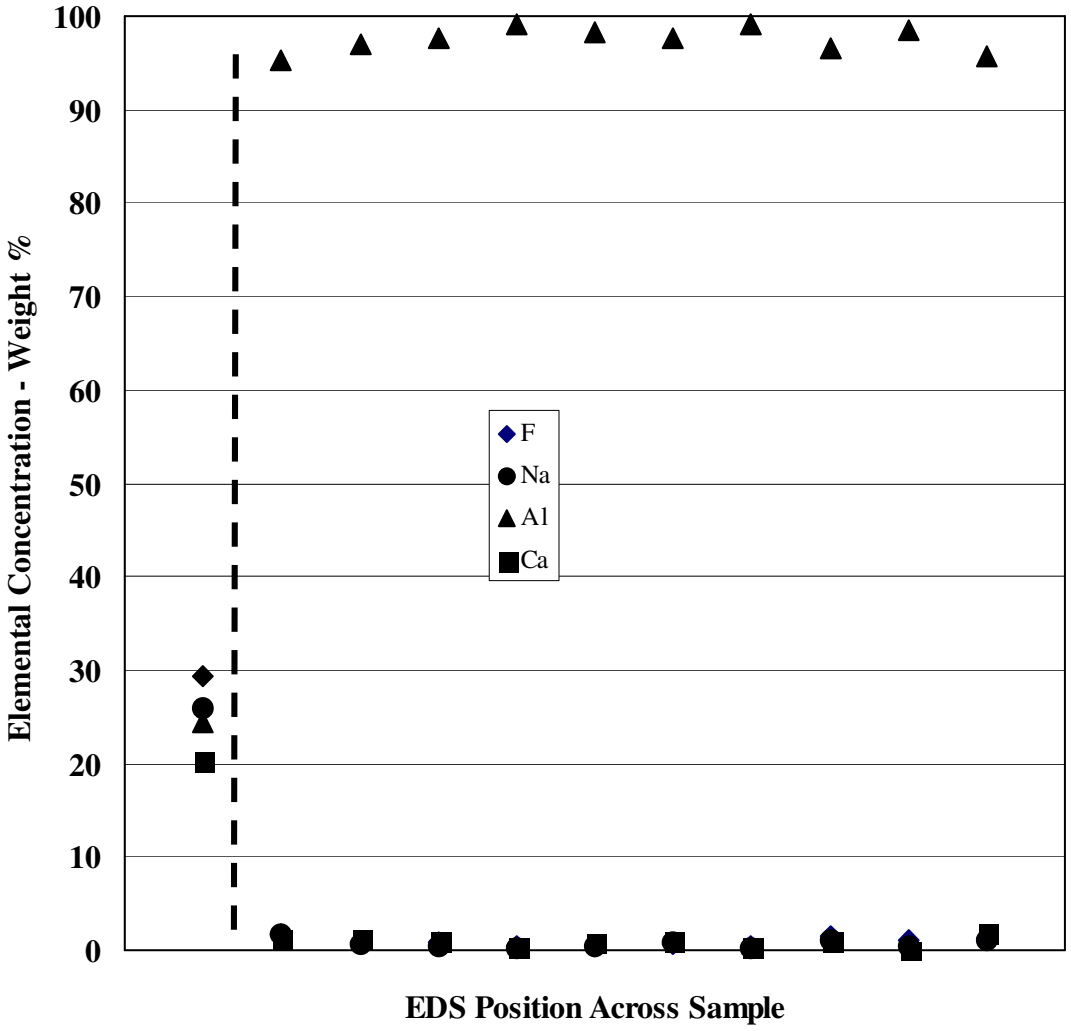

Figure 16. Results of equi-distance EDS analyses made across the used dense alumina ball section shown in Figure 15. EDS results obtained to the left of vertical dashed line were made inside the adhering bath layer. EDS results to the right of the vertical dashed line were made inside the dense alumina ball.